Bacteria and Viruses in Arctic Sea Ice

Andrey F. Sazhin [1, 2], Nadezhda D. Romanova [1, 2], Alexander I. Kopylov [3], Elena A. Zabotkina [3]

[1] Shirshov Institute of Oceanology, Russian Academy of Sciences, Moscow 117997, Russia

[2] Obukhov Institute of Atmospheric Physics, Russian Academy of Sciences, Moscow 119017, Russia.

[3] Papanin Institute for Biology of Inland Waters, Russian Academy of Sciences, Borok 152742, Russia

Corresponding Author:

Andrey F. Sazhin [1, 2]

Email address: andreysazhin@yandex.ru

PeerJ Preprints | https://doi.org/10.7287/peerj.preprints.26607v1 | CC BY 4.0 Open Access | rec: 3 Mar 2018, publ: 3 Mar 2018

Abstract

We studied vertical distribution of bacteria and viruses in different layers of the Arctic sea ice drilled at the North Pole. The sampled multi-year ice was characterized by uneven vertical distribution of bacterial abundance. This characteristic varied within the range of 8±1.2 $\times 10^3$ to 95±2.6 $\times 10^3$ cells ml^{-1}. The average bacterial abundance was 28±2.9$\times 10^3$ cells ml^{-1}. The layers with the maximal bacterial abundance were located in the intermediate and lower layers of the ice cores. The morphological composition of bacterial population of the multi-year ice was dominated by the cocci cells (63-92%). Bacterial population of the multi-year ice consisted of rather large cells with the mean cell volume of 0.14 μm^3. Bacterial biomass varied from 0.5 to 5 mg C m^{-3} with the mean value 1.57±0.2 mg C m^{-3}. The vertical distribution of bacterial biomass generally followed the pattern of bacterial abundance distribution. The maximal viral abundance was also located in the upper, intermediate and lower layers of the ice. The ratio of viral to bacterial abundance varied from 0.6 to 28, with the mean value 12.5. The average total number of phages attached to bacteria was 6.2 $\times 10^3$ viral particles ml^{-1}. The fraction of viruses attached to bacteria varied from 0.5 to 20.7%, with the mean value 7.1% of the total viral abundance. The number of bacterial cells with viral particles attached to them varied from 0.7 to 32$\times 10^3$ cells ml^{-1}, with the mean value 8$\times 10^3$ cells ml^{-1}. The number of viral particles located within bacterial cells varied from 2 to 21 particles per a bacterial cell. The minimum and maximum numbers of viruses located on bacterial cells varied from 1 to 6 viral particles per a bacterial cell. The mean viral capsid size varied from 42 to 83 nm. The frequency of visibly infected bacterial cells (*FVIC*) calculated for the upper, intermediate and lower layers of the ice was 0.92, 1.23 and 0.8% of the total viral abundance, respectively. The overall frequency of infected cells (*FIC*) calculated for the same layers was 6.3, 8.4 and 0.8% of the viral numbers, respectively, while the viral-mediated mortality of bacteria (*VMB*) was 7.1, 9.8 and 6.1 %, respectively. The average number of viral particles located within bacterial cells was 7.3 particles per a cell. Our data show that during the study period the rate of viral infection of bacterial cells and the viral-mediated mortality of bacterial cells in the multy-year ice of the North Pole were relatively low.

Introduction

Sea ice is a unique ecosystem in the Arctic, providing habitat to specialized ice-associated organisms that include bacteria and viruses – the smallest and most abundant species of the community. These groups not only use the ice as their habitat, the interactions that take place between them have a potentially great effect on the functioning of the whole ecosystem. To be more specific, the virus-induced bacterial lysis results in the release of bacterial carbon into the environment that either transferred to the upper trophic levels when consumed by protozoa and multicellular filter feeders or, alternatively, contribute to the dissolved organic matter stocks (Weinbauer, 2004; Kopylov, Kosolapov, 2011) Thus, the dramatic reduction in the summer extent of Arctic sea ice affects biological and biogeochemical processes operating at the ice-ocean-atmosphere interfaces, as well as throughout the water column. We do not know what these new Arctic conditions mean for the marine biota (Bluhm et al. 2015). The interconnections between the sea ice melt and trophic changes at the base of the Arctic marine food web, including the potential impact on the species of sea ice biota are poorly studied and several fundamental questions remain elusive. Will the production at these lower trophic levels increase or decrease with the sea ice coverage and extent reducing over time and space? Will biodiversity of the Arctic ecosystems shift to the "sub-arctic" state and will the Arctic marine food web provide more or less energy for the higher trophic levels as a result?

The unprecedented warming of the Arctic Ocean over the past three decades has resulted in the reduction of the sea ice extent (Cavalieri & Parkinson, 2012) and thickness (Kwok et al., 2009), as well as the decline in the amount of multi-year ice (Comiso, 2012). Here, we address the potential effects of the reduction of sea ice coverage on the marine food web functioning by examining the structure of the microbial community of the multi-year ice.

Materials and Methods

The first multi-year ice core was drilled on 13 April 2007 at the North Pole (camp «Peter», Station 1: N 89° 29', E 22° 49') during the "PALEX" pan arctic ice expedition. The second ice core was drilled on 2 August 2007 at the North Pole during the 26th voyage of the RV "Akademik Fyodorov" (N 89° 59'5", E 49° 04'00"). The third core was drilled on 13 April 2015 at the North Pole-2015 drifting ice station (N 89° 30'27", E 20° 24'13").

The ice cores were drilled using a titanium ice auger (diameter: 140 mm). The frozen cores placed in sterile plastic tubes were then delivered to Moscow for further data analysis. The multi-year ice cores were then cut into consecutive segments, 12-25 cm in length each, although the length of a given segment could be adjusted so that the pattern of visually distinct layers could be followed correctly. Three samples were taken from the first-year ice (Core 3) collected at the North Pole: from the upper (3 to 7 cm), intermediate (80 to 90 cm) and the lower (162 to 166 cm) layers. An additional water sample was taken directly from beneath the sea ice.

Ice samples were allowed to melt in the dark at 1 to 4 °C and were then fixated with 1% formaldehyde solution. Bacterial abundance was estimated from samples stained with DAPI using direct counting under an epifluorescent microscope (Porter, Feig, 1980; Hoff, 1993). Bacterial cell volume was calculated from the linear dimensions of a given cell measured with an eyepiece micrometer. Bacterial carbon biomass was estimated using the following equation:

$$fgC/cell = 133{,}754 \times V^{0{,}438},$$

where *fgC/cell* is the cell carbon content (in femtograms), V – the bacterial cell biovolume (μm^3) (Romanova, Sazhin, 2010).

The analysis of concentration of viral particles (Vp) was additionally performed for the ice samples from Core 1. Transmission electron microscopy was used in order to estimate the following characteristics: the number of free viral particles, the number of phages attached to bacterial cells, the frequency of visibly infected cells (*FVIC*, measured as the fraction of the total number of bacteria) and the mean number of matured phages in the virus-infected bacterial cells (i.e. the burst size, *BS*, Vp/cell) (Zheng et al., 1996). Viruses and bacteria were centrifuged at 100 000 g (35 000 rpm) for two hours using the OPTIMA L-90k ultracentrifuge (Beckman Coulter, USA) on Pioloform/carbon-coated 400-mesh nickel grids. The grids were further analysed under a JEM 1011 electron microscope (Jeol, Japan) at ×50000–150000 magnification. Not less than 800 free virus particles and 800 bacterial cells were analysed for each grid.

To calculate the overall frequency of infected bacterial cells from the total bacteria cell number (i.e. *FIC*), we used the following equation (Binder, 1999):

$$FIC = 7.1 \times FVIC - 22.5 \times FVIC^2.$$

Virus-mediated mortality of bacteria (*VMB*), i.e. the fraction that the virus-induced mortality makes of the total bacterial mortality or production, was estimated as (Binder, 1999):

$$VMB = (FIC + 0.6 \times FIC^2) / (1 - 1.2 \times FIC)$$

The absolute values of both *FVIC* and *FIC* were used. According to this approach the bacterial production is assumed to be equal to the total mortality of bacterioplankton.

Results

Core 1. Second-year ice that is 192 cm thick. In the upper 25 cm layer the ice is formed by firn, is white in colour, opaque, solid and monolithic, with pores 1 to 3 mm in diameter. Further down to 180 cm deep, the ice is grey, semi-transparent, solid and monolithic, with occasional pores 1 to 3 mm in diameter. Within the 180 to 192 cm layer the ice is also grey, semi-transparent, but here it is semisolid and has characteristic brine channels together with occasional pores 1 to 5 mm in diameter, as well as oblong caverns.

Core 2. Second-year ice that is 225 cm thick. The upper 25 cm layer of the ice core is formed by firn, is grey, opaque, semi-soft, with pores 1 to 2 mm in diameter. Further, down to the 90 cm layer the ice is whitish-grey, opaque, lacks the well-developed brine channels. Deeper the ice is white, solid, has well-developed brine channels. Vertical structuring of the layer (bands) is practically lacking. At the layers located from 90 to 225 cm the ice is whitish-grey, uniform, the brine channels are better developed, pores of about 1 mm in diameter are present. At the lowest layer the size of the brine channels increases compared to those at the upper layers.

Core 3. First-year ice that is 180 cm thick. Three layers can be clearly defined in the core. Upper layer (from 0 to 50 cm) is formed by blueish-grey opaque, crystalline ice, with heterogeneous whitish streaks of different intensity. Pores are present in the streaks that are generally up to 1 mm in diameter. The intermediate layer (from 50 to 160 cm) has a more uniform structure. Here the ice is predominantly microcrystalline, whitish-grey in colour, semi-transparent with numerous pores that are up to 5 mm in diameter. The pores form clusters of various shape, as well as vertical chains that are up to 10 cm in length. Vertical brine channels that are up to 3 cm

in length appear in the lower part of this layer. The lower layer (from 160 to 180 cm) is formed by blueish-grey ice that is opaque and heterogeneous in structure. The ice becomes progressively crumbly in texture and cavernous as one approaches the bottom of the layer. In the middle of this third layer (from 162 to 172 cm) numerous cavities and air bubbles that are up to 3 mm in size and form a branched system are located. The lowest section of the core (from 172 to 180 cm) is formed by macro-crystalline ice of irregular shape.

Bacteria.

The sampled multi-year ice was characterized by uneven vertical distribution of bacterial abundance (Fig.1). This characteristic varied within the range of 21 to 68±3.2 $\times 10^3$ cells ml^{-1} (Core 1) and 8±1.2 $\times 10^3$ to 95±2.6 $\times 10^3$ cells ml^{-1} (Core 2). Thus, the bacterial cell numbers could differ as much as 12 times between certain parts of the cores. The average bacterial abundance was 28±2.9 $\times 10^3$ cells ml^{-1}. The layers with the maximal bacterial abundance in the two cores were located at the depth of 110 to 125 cm (the intermediate part of both Core 1 and Core 2) and 210 to 225 cm (bottom of Core 2): 68-72±6.2 $\times 10^3$ cells ml^{-1} and 95±7.7 $\times 10^3$ cells ml^{-1}, respectively. These maxima most likely reflect the seasonal peaks of bacterial abundance in summer. The maximal concentrations of dissolved organic carbon (DOC) are also characteristic of the abovementioned layers, with the values of 1.3 to 1.4 mgC l^{-1}, while the average DOC concentration in the remaining layers is 1.0 mgC l^{-1} (Belyaev, personal communication).

The morphological composition of bacterial population of the multi-year ice was dominated by the cocci cells (63-92%). However, the rod-shaped cells can make more than 50% of bacterioplankton in the upper 50 cm of the ice (Fig. 1; Core 2). It should also be noted that the fraction of rod-shaped bacteria increased in the upper part of the core (15-23% in the layer 0-120 cm compared to 7-15% in the layer 120-225 cm). Bacterial population of the multi-year ice consisted of rather large cells (the mean cell volume: 0.14 μm^3). Bacteria with the maximum cell size were located in the upper part of the ice core (0.24 μm^3; Core 2). Bacterial biomass in the multi-year ice cores varied from 1 to 4.2±1.7 mg C m^{-3} (Core 1) and from 0.5 to 5 mg C m^{-3} with the mean value of 1.57±0.2 mg C m^{-3} (Core 2). The vertical distribution of bacterial biomass generally followed the pattern of bacterial abundance distribution. The maximum values of bacterial biomass were observed in the layers located at 110-125 cm for both Core 1 and Core 2 (4.2-5±0.4 mg C m^{-3}) and at 210-225 cm of Core 2 (4.5 ±0.4 mg C m^{-3}). However, it should be

noted that relatively high values of bacterial biomass (1.93±0.2 mg C m^{-3}) were observed in the upper layers of both cores (Fig.1).

Bacterial distribution in the first-year ice sampled in 2015 (Core 3) slightly differed from that in the two second-year ice cores sampled in 2007 (Cores 1 and 2). The abundance of bacterial cells in the upper layer was comparatively higher with the mean value 53±4.5 $\times 10^3$ cells ml^{-1} that combined with similar bacterial biomass values for the cores: 2.06±0.2 mg C m^{-3}. In the intermediate layers bacterial abundance reached 60±6.7 $\times 10^3$ cells ml^{-1} (1.09±0.1 mg C m^{-3}). In the lower layers of the ice Core 3 the concentration of bacteria was relatively low (25±0.3 $\times 10^3$ cells ml^{-1} or 0.95±0.01 mg C m^{-3}) and matched the bacterial abundance in the lower layers of Core 1. The abundance of bacteria in the samples of water taken directly from beneath the sea ice was close to the abundance values characteristic of the upper and intermediate layers and was 51±3.7 $\times 10^3$ cells ml^{-1} or 0.97±0.07 mg C m^{-3}. Similarly to the two cores drilled in 2007, the distribution of different morphological types of bacteria in Core 3 was as follows: 79-87% were cocci cells, 10-16% were the rod-shaped cells, 0.4-4.6% - other morphological groups. Population of bacteria of the first-year ice consisted of small cells (mean cell volume 0.05 μm^3).

Viruses.

The number of viruses in different layers of the ice Core 1 was 17-952$\times 10^3$ Vp ml^{-1} (Table 1).The maximal viral abundance was located in the upper, intermediate and lower layers of the ice core, although these maxima did not exactly correspond to the vertical distribution of the maxima of bacterial abundance. The ratio of viral to bacterial abundance varied from 0.6 to 28, with the mean value 12.5. The average total number of phages attached to bacteria in the ice Core 1 was 6,2 $\times 10^3$ Vp ml^{-1} with the value varying between different core layers from 1.4 to 11.8 $\times 10^3$ Vp ml^{-1}. The fraction of viruses attached to bacteria varied from 0.5 to 20.7%, with the mean value 7.1% of the total viral abundance. The number of bacterial cells with viral particles attached to them varied from 0.7 to 32$\times 10^3$ cells ml^{-1}, with the mean value 8$\times 10^3$ cells ml^{-1}. Thus, the average fraction of bacterial cells with viral particles attached to them of the total number of bacteria was 18%, with the variation of the values from 3.1 to 32%. The minimum and maximum numbers of viruses located on bacterial cells in different ice layers varied from 1 to 6 viral particles, with the mean value for the core 1.4 viral particles per a bacterial cell (Table 1).

The capsid size of the viral particles varied considerably: from 24 to 187 nm, with the maximum dispersion of the values characteristic of the layer located at the depth of 160 to 180 cm (Table 2). Within the limits of each layer of Core 1, the mean capsid size varied from 42 to 83 nm, while the average value for the whole core was 60 nm. The data on the size distribution of the viruses and the total abundance of the size groups are given in Table 2. As it can be seen from the table, the majority of the viral particles were those with the capsid size from 40 to 100 nm. Viruses with the capsid size exceeding 200 nm were absent from the analysed samples.

The data on the frequency of visibly infected bacterial cells (*FVIC*), frequency of infected cells (*FIC*) and viral-mediated mortality of bacteria (*VMB)* are given in Table 3. The *FVIC* values calculated for the upper, intermediate and lower layers were 0.92, 1.23 and 0.8% of the total viral abundance, respectively. The *FIC* values calculated for the same layers were 6.3, 8.4 and 0.8% of the viral numbers, respectively, while *VMB* was 7.1, 9.8 and 6.1% respectively, of the overall bacterioplankton mortality, respectively. The number of viral particles located within bacterial cells (i.e. burst size, *BS*) varied from 2 to 21 particles per bacterial cell. The maximal rate of virus-induced infection of bacterioplankton was characteristic of the lower layer (located at the depth of 160 to 180 cm) of Core 1. The average *BS* value calculated for the whole ice core was 7.3 Vp $cell^{-1}$.

Discussion

Bacterial abundance was analysed both in the water and ice samples from the Polar Region by quite a number of authors (Maranger et al.,1994; Meiners et al., 2003; Stewart, Fritsen, 2004; Wells & Deming, 2006). In our study the average number of bacteria located in the ice did not exceed that in the samples of water taken directly from beneath the ice. The similar values of bacterial abundance in the ice and water samples for 2015 are most likely the result of similarity in the conditions affecting the bacterioplankton population in the two types of environment The multi-year ice was characterized by an uneven vertical distribution of bacterial abundance. Two peaks of bacterial abundance were observed in the middle and lower layers of the ice. The increase in bacterial abundance in the intermediate layers of the ice most likely reflects the seasonal peaks of bacterial numbers in summer. Unfortunately, there are very few data on the pattern of vertical distribution of bacteria and viruses between the Arctic ice layers of different origin and structure. However, the seasonal pattern of bacterial vertical distribution was

provided by a number of authors (Maranger et al., 1994; Kottmeier, Sullivan, 1990; Delille et al., 2002; Collins et al., 2008). Notably, a pattern of vertical distribution of bacteria from multi-year ice that was similar to the one described in our work, was found in the pack ice from other regions of the Arctic Ocean (Gradinger, Zhang, 1997; Junge et al., 2002).

Bacterial abundance in the center of the Arctic Ocean was significantly lower than the values reported by other researchers who worked in the regions of ice formation and outlet from the Transpolar Drift Stream: in the Chukchi Sea, the Beaufort Sea and the Fram Strait (Kaneko et al., 1977; Junge et al., 2002; Brinkmeyer et al., 2003; Meiners et al., 2003). This might suggest that bacterial abundance in the pack ice may change depending on the region of location of the ice, while the pattern of vertical distribution of bacterial numbers remains unchanged. The fact that in the abovementioned studies bacterial abundance in the water from beneath ice was close to the average bacterial numbers in the ice core may confirm this assumption. Our results together with the data from the previous studies allow one to assume that bacterial growth and distribution in ice do not follow any consistent pattern and are most likely dependent on location of spots of available organic matter. This pattern of distribution is generally maintained during the initial part of the transition from the winter heterotrophic microbial community to the phototrophic community in the springtime. In the course of further development of the sea ice microbial community the maximum bacterial activity tends to coincide with the bottom layer that is enriched with available organic matter due to the algal bloom. In multi-year ice this pattern may occur several times following the consecutive seasonal changes. Eventually, in the multi-year ice a stratified pattern of bacterial vertical distribution that correlates with that of chlorophyll *a* can be observed (Gradinger, Zhang, 1997). Bacterial abundance in multi-year ice is to a high extent determined by the route along which the ice drifts, since it is affected by bacterial numbers in the water beneath the ice. Nevertheless, the general pattern of the vertical distribution of bacteria in the ice remains the same: the peaks of bacterial abundance located in the layers associated with the summer algal bloom separate the zones where bacterial abundance matches that in the water from beneath the ice.

Seasonal variations in the abundance of bacteria may be caused by several factors. First, the slowing down of bacterial growth during the transition from the heterotrophic winter microbial community to a phototrophic spring community (Meiners et al. 2002, Terrado et al., 2008). Apart from that, the decrease in bacterial numbers during winter may be attributed to the

brine rejection and the viral lysis induced by high concentrations of both bacterial and viral particles in brine water (Collins et al., 2008).

Relatively few samples of sea ice have been examined under microscope in order to make relevant quantifications, with the majority of the samples taken in the Ross Sea (Maranger et. al., 1994; Gowing et al., 2002, 2004; Gowing, 2003;) and only a single sample from the Arctic (Wells & Deming, 2006).

In the cold waters from a variety of biotopes of the Arctic Ocean the viral-induced mortality of bacteria can vary from less than 1% to 100% of the daily bacterial production (Guixa-Boixereu et al., 2002; Wells, Deming, 2006, Steward et al., 2007). Most often the values of viral-mediated mortality of bacteria vary from 1% (Steward et al., 2007) to 50.6% of bacterial production (Boras, 2010). During our study at the North Pole the rate of viral infection and viral-mediated mortality of bacteria were shown to be relatively low. The mean values of *FVIC* and *VMB* were 1% and 8%, respectively.

Conclusion

Two peaks of bacterial and viral abundance were located in the intermediate and bottom layers of the Arctic ice. The increase in the number of bacteria in the intermediate layers of the ice most likely reflect the summer peaks of bacterial abundance in the first year, when these layers were located at the bottom of the ice, and the summer algal bloom took place. Therefore, the vertical distribution of bacteria is most likely determined by the distribution of local spots of available organic matter. In the intermediate and lower ice layers the bacteria numbers are associated with the organic matter enrichment due to the algal bloom in spring and summer of the second year. The increase in concentration of viral particles in the intermediate and lower layers of the ice directly follows the peaks of bacterial abundance in these layers. Moreover, the numbers of bacteria and, consequently, viruses in the lower layers of ice is linked to the bacterial and viral abundance in the thin layer of water just beneath the ice. During our study at the North Pole the rate of viral infection (1%) and the viral-mediated mortality of bacteria (8 %) were shown to be relatively low.

Acknowledgements

The authors thank A.N. Novigatsky, N.A. Belyaev and L. E. Reykhard for providing the ice cores used in the study.

Funding

This study was supported by the Russian Ministry of Education and Science, agreement number 14.616.21.0078 (RFMEFI61617X0078).

References

Binder B. 1999. Reconsidering the relationship between virally induced bacterial mortality and frequency of infected cells. *Aquatic Microbial Ecology* 18: 207-215.

Bluhm B.A., Kosobokova K.N., Carmack E.C. 2015. A tale of two basins: An integrated physical and biological perspective of the deep Arctic Ocean. *Progress in Oceanography* 139:89-121.

Boras J.A., Sala M.M., Arrieta J.M., Sà E.L., Felipe J., Agustí S., Duarte C.M., Vaquéet D. Effect of ice melting on bacterial carbon fluxes channeled by viruses and protists in the Arctic Ocean. *Polar Biology* 33:1695–1707.

Brinkmeyer R., Knittel K., Jürgens J.,Weyland H., Amann R., Helmke E. 2003. Diversity and Structure of Bacterial Communities in Arctic versus Antarctic Pack Ice. *Applied and Environmental Microbiology* 69(11): 6610-6619.

Cavalieri D.J., Parkinson C.L. 2012. Arctic sea ice variability and trends, 1979–2010. *The Cryosphere* 6: 881–889.

Collins R.E., Carpenter Sh. D., Deming J.W. 2008. Spatial heterogeneity and temporal dynamics of particles, bacteria, and pEPS in Arctic winter sea ice. *Journal of Marine Systems* 74: 902-917.

Comiso J.C., 2012. Large decadal decline of the Arctic multiyear ice cover. *Journal of Climate* 25: 1176–1193.

Delille D., Fiala M., Kuparinen J., Kuosa H., Plessis Ch. 2002. Seasonal changes in microbial biomass in the first-year ice of the Terre Adélie area (Antarctica). *Aquatic Microbial Ecology* 28: 257-265.

Hoff K.A. 1993. Total and specific bacterial counts by simultaneous staining with DAPI and flourochrome-labeled antibodies. *Handbook of methods in Aquatic microbial ecology*. Lewis Publishers. 149-154.

Gowing M.M. 2003. Large viruses and infected microeukaryotes in Ross Sea summer pack ice habitats. *Marine Biology* 142: 1029-1040.

Gowing M.M., Garrison D.L., Gibson A.H., Krupp J.M., Jeffries M.O. Fritsen C.H. 2004. Bacterial and viral abundance in Ross Sea summer pack ice communities. *Marine Ecology Progress Series* 279: 3-12

Gowing M.M., Riggs B.E., Garrison D.L., Gibson A.H., Jeffries M.O. 2002. Large viruses in Ross Sea late autumn pack ice Habitats. *Marine Ecology Progress Series* 241: 1-11.

Gradinger R., Zhang Q. 1997. Vertical distribution of bacteria in Arctic sea ice from the Barents and Laptev Seas. *Polar Biology* 17: 448-454.

Guixa-Boixereu N., Vaqué D., Gasol J.M., Sánchez-Cámara J., Pedrós-Alió C. 2002. Viral distribution and activity in Antarctic waters. *Deep Sea Res II* 49: 827-845.

Junge K., Imhoff F., Staley T., Deming J.W. 2002. Phylogenetic diversity of numerically important Arctic sea-ice bacteria cultured at subzero temperature. *Microbial Ecology* 43(3): 315-328.

Kaneko T., Roubal G., Atlas R.M. 1977. Bacterial populations in the Beaufort Sea. *Nature* 270: 596–599.

Kopylov A.I., Kosolapov D.B. 2011. Microbial loop in freshwater and marine plankton ecosystems. Izhevsk: KnigoGrad. 332p. (Mikrobnaya petlia v planktonnih soobshestvah morskih i presnovodnih ekosistem. Izhevsk: KnigoGrad (in Russian)).

Kottmeier S.T., Sullivan C.W. 1990. Bacterial biomass and production in pack ice of Antarctic marginal ice edge zones. *Deep Sea Research* 37(8): 1311-1330.

Kwok R., Cunningham G.F., Wensnahan M., Rigor I., Zwally H.J., Yi D. 2009.Thinning and volume loss of the Arctic Ocean sea ice cover: 2003–2008. *Journal of Geophysical Research* 114 (C7): 1-16. http://dx.doi.org/10.1029/2009jc005312.

Leeuwe M.A., Tedesco L., Arrigo K.R., Assmy P., Campbell K., Meiners K.M., Rintala J.M., Selz V., Thomas D.N., Stefels J. 2018. Microalgal community structure and primary production in Arctic and Antarctic sea ice: A synthesis. *Elementa Science of the Anthropocene* 6:4. DOI: https://doi.org/10.1525/elementa.267.

Maranger R., Bird F.D., Juniper S.K., 1994. Viral and bacterial dynamics in Arctic sea ice during the spring algal bloom near Resolute, N.W.T., Canada. *Marine Ecology Progress Series* 111:121-127.

355 Meiners K., Fehling J., Granskog M.A. Spindler M., 2002. Abundance, biomass and composition
356 of biota in Baltic sea ice and underlying water (March 2000). *Polar biology* 25:7 61-770.
357 Meiners K., Gradinger R., Fehling J., Civitarese G., Spindler M., 2003. Vertical distribution of
358 exopolymer particles in sea ice of the Fram Strait (Arctic) during autumn. *Marine Ecology*
359 *Progress Series* 248: 1-13.
360 Porter K.G., Feig Y.S. 1980. The use of DAPI for identifying and counting aquatic microflora.
361 *Limnology and Oceanography* 25(5): 943-948.
362 Romanova N.D., Sazhin A.F. 2010. Relationships between the cell volume and the carbon
363 content of bacteria. *Oceanology* 50 (4): 522–530. DOI: 10.1134/S0001437010040089.
364 Steward G.F., Fandino L.B., Hollibaugh J.T., Whitledge T.E., Azam F. 2007. Microbial biomass
365 and viral infections of heterotrophic prokaryotes in the sub-surface layer of the Central Arctic
366 Ocean. *Deep Sea Research I.* 54: 1744−1757.
367 Stewart F.J., Fritsen C.H. 2004. Bacteria-algae relationships in Antarctic sea ice. *Antarctic*
368 *science* 16 (2): 143-156.
369 Terrado R., Lovejoy C., Massana R., Vincent W.F. 2008. Microbial food web responses to light
370 and nutrients beneath the coastal Arctic Ocean sea ice during the winter-spring transition.
371 *Journal of Marine Systems* 74: 964-977.
372 Wells L.E., Deming J.W. 2006. Modelled and measured dynamics of viruses in Arctic winter sea
373 ice brines. *Environmental Microbiology* 8: 1115-1121.
374 Weinbauer M.G. Ecology of prokaryotic viruses. 2004. FEMS Microbiology Reviews 28(2):
375 127−181.
376 Zheng Y. Z., Web R., Greenfield P.F., Reid S. Improved method for counting virus and virus
377 like particles. 1996. *Journal of Virological Methods* 62: 153-159.
378

Figure 1(on next page)

Vertical distribution of bacterial numbers and biomass in the multi-year ice

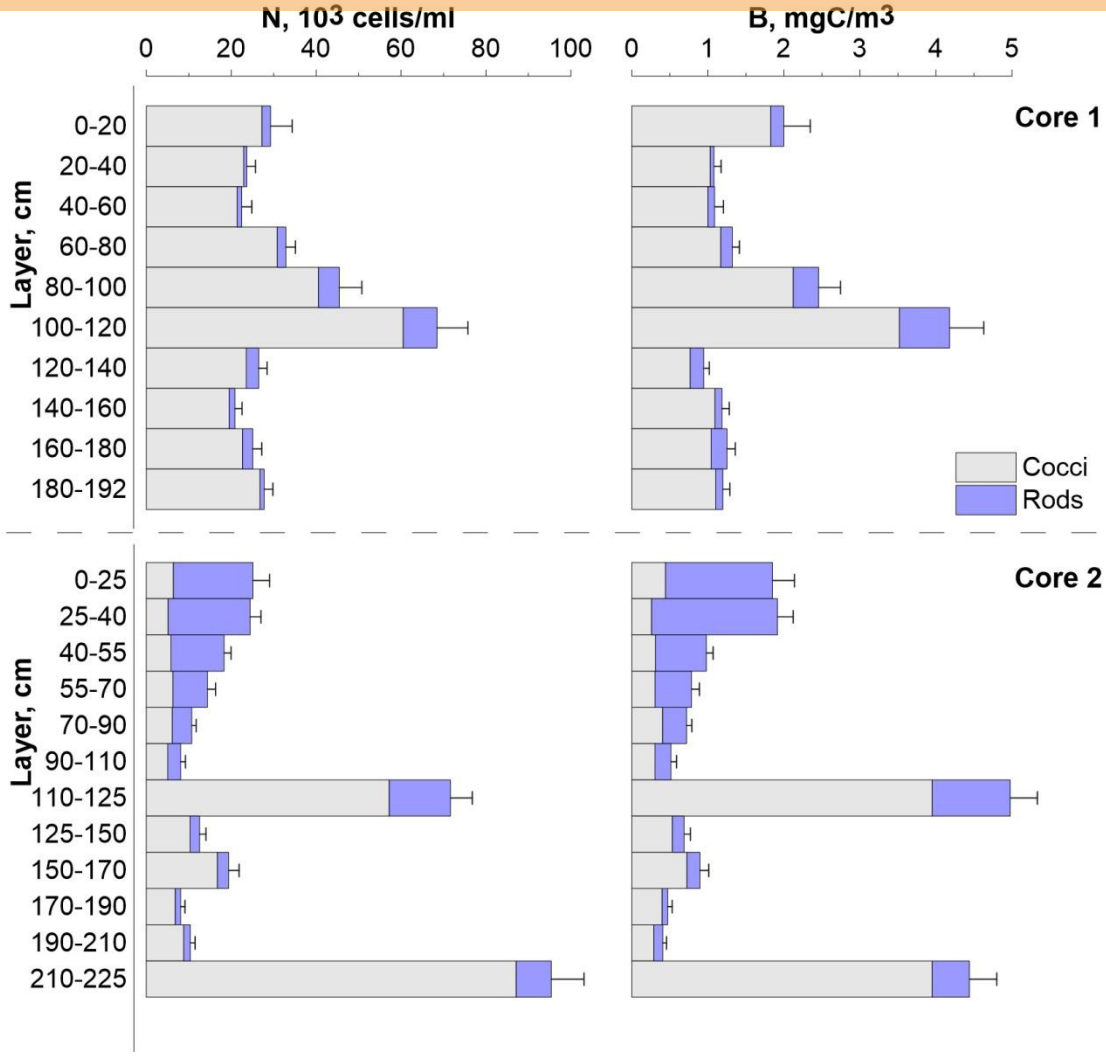

Figure 1. Vertical distribution of bacterial numbers (N) and biomass (B) in the multi-year ice

Table 1(on next page)

Characteristics of viruses and bacteria from different layers of ice

Table 1. Characteristic of viruses (viruses particles, Vp) and bacteria (B) from different layers of ice[1]

Layer (cm)	N_V	N_B	N_V/ N_B	N_{VB}	N_{VB}/ N_V	N_{BV}	N_{BV}/ N_B	N_{VBC}	$N_{VBC\ AVG}$
0-20	53	29	1.8	5.32	10.1	5.32	18.2	1.0	1±0
20-40	514	24	21.7	4.96	1.0	4.10	17.3	1-3	1.21±0.05
40-60	17	22	0.8	1.40	8.0	0.70	3.1	2	2±0
60-80	24	33	0.7	4.98	20.7	3.98	12.1	1-2	1.25±0.05
80-100	952	45	21.0	4.57	0.5	3.09	28.7	1-4	1.48±0.07
100-120	58	68	0.8	7.42	12.8	4.95	7.2	1-2	1.5±0.05
120-140	17	26	0.6	7.56	4.5	6.30	23.8	1-2	1.2±0.04
140-160	156	21	7.5	6.14	3.9	4.91	23.5	1-2	1.25±0.05
160-180	703	25	28.0	11.79	1.7	31.99	32.0	1-6	1.47±0.08
180-192	91	28	3.3	7.34	8.0	14.71	14.7	1-3	1.8±0.08

[1] The total number of all groups of viruses (N_V, $\times 10^3$ Vp ml^{-1}), the number of bacteria (N_B, $\times 10^3$ cells ml^{-1}), the ratio of viral to bacterial abundance (N_V/N_B), the number of viruses attached to bacterial cells (N_{VB}, $\times 10^3$ Vp ml^{-1}) and the fraction that the viral particles attached to bacterial cells make of the total abundance of the viruses (N_{VB}/N_V, %), the number of bacterial cells that have viral particles attached to them (N_{BV}, $\times 10^3$ cells ml^{-1}), the fraction that bacteria with attached viral particles make of the total bacterial abundance (N_{BV}/N_B, %), the minimum and maximum number of viral particles locates on a bacterial cell (N_{VBC}), the mean number of viral particles locates on a bacterial cell ($N_{VBC\ AVG}$).

Table 2(on next page)

Capsid diameter of the viral particles of different size groups

Table 2. Capsid diameter of the viral particles of different size groups from different layers of ice[1]

Layer (cm)	D	D_{AVG}	S_V				
			< 40	40-60	60-100	100-150	150-200
			N_{VS}				
0-20	37-158	62±4	9.1	54.6	27.3	4.5	4.5
20-40	26-140	66±6	5.9	41.2	44.1	8.8	0
40-60	25-64	42±4	33.3	55.6	11.1	0	0
60-80	29-101	54±4	25.0	43.8	25.0	6.2	0
80-100	29-174	83±8	7.1	30,4	30.3	28.6	3.6
100-120	40-72	52±4	9.1	63.6	27.3	0	0
120-140	40-85	54±4	0	53.9	38.5	7.7	0
140-160	26-114	68±6	5.3	36.8	44.7	13.2	0
160-180	24-187	64±8	26.5	22.6	39.6	9.4	1.9
180-192	26-100	51±5	45.5	18.2	36.3	0	0

[1]The minimum and maximum viral capsid diameter (D, nm), the average viral capsid diameter ($D_{AVG,}$ nm), the fraction that the viral particles of different size groups (S_V, nm) make of the total number of viruses ($N_{VS,}$ %) in different layers of ice.

Table 3(on next page)

Characteristics of visibly infected bacterial cells from different layers of ice

PeerJ Preprints | https://doi.org/10.7287/peerj.preprints.26607v1 | CC BY 4.0 Open Access | rec: 3 Mar 2018, publ: 3 Mar 2018

Table 3. Characteristic of visibly infected bacterial cells from different layers of ice[1]

Layer (cm)	*FVIC*	*FIC*	*VMB*	*BS*	BS_{AVG}
0-20	0	0	0	0	0
20-40	0.92	6.30	7.10	2-8	4.75±1.60
40-60	0	0	0	0	0
60-80	0	0	0	0	0
80-100	1.23	8.40	9.80	3-12	7.20±1.63
100-120	0	0	0	0	0
120-140	0	0	0	0	0
140-160	0	0	0	0	0
160-180	0.80	0.80	6.10	3-21	10.0±6.41
180-192	0	0	0	0	0

[1]The frequency of visibly infected bacterial cells (*FVIC*, % N_B), the overall frequency of infected bacterial cells (*FIC*, % N_B), viral-mediated mortality of bacteria (*VMB*, % P_B), the number of viruses located within bacterial cells: the minimum and maximum values (burst size, *BS*, Vp/cell), and the mean value ($BS_{AVG,}$ Vp/cell) in different layers of ice.